Ground-based network observation of Asian dust events of April 1998 in east Asia

Toshiyuki Murayama,[1] Nobuo Sugimoto,[2] Itsushi Uno,[3] Kisei Kinoshita,[4]
Kazuma Aoki,[5] Naseru Hagiwara,[1] Zhaoyan Liu,[2] Ichiro Matsui,[2] Tetsu Sakai,[6]
Takashi Shibata,[6] Kimio Arao,[7] Byung-Ju Sohn,[8] Jae-Gwang Won,[9]
Soon-Chang Yoon,[9] Tao Li,[10] Jun Zhou,[10] Huanling Hu,[10] Makoto Abo,[11]
Kengo Iokibe,[12] Ryuji Koga,[12] and Yasunobu Iwasaka[6]

Abstract. We coordinated a ground-based network that has been in use since 1997 to observe Asian dust during springtime. Huge Asian dust events that occurred in the middle of April 1998 were captured by this network. In this paper we present the organization of the network; a description of the instruments, including the lidar, sky radiometer, and optical particle counter; and the results of the observation, and offer discussions regarding the transport mechanism of Asian dust in east Asia using an on-line tracer model. We discussed the time series of the surface concentration and the height distribution of the dust. A cutoff cyclone generated during the dust episode was responsible for trapping and sedimentation during the transportation of the Asian dust, particularly in the southern parts of China and Japan. Horizontal dust images derived from NOAA/AVHRR clearly revealed the structure of the vortex. The lidar network observation confirmed the general pattern of dust height distribution in this event; the height of the major dust layer was about 3 km over Japan but was higher (4 to 5 km) in Seoul and Hefei. A thin dust layer in the upper troposphere was also commonly observed in Hefei and Japan. Evidence of the coexistence of dust and cirrus was shown by the polarization lidar. The lidar network observation of Asian dust and satellite remote sensing provide key information for the study of the transport mechanism of Asian dust. Further extension of the lidar network toward the interior of the continent and the Pacific Rim would reveal the greater global mechanism of the transportation.

1. Introduction

Asian dust is commonly called "yellow sand" in China, Korea, and Japan in their languages of Huang Sha, Hwang Sa, and Kosa. It is a well-known phenomenon during the spring season in east Asia. In fact, Asian dust has been a matter of

[1]Department of Physics, Tokyo University of Mercantile Marine, Koto, Tokyo, Japan.
[2]Atmospheric Environment Division, National Institute for Environmental Studies, Tsukuba, Ibaraki, Japan.
[3]Research Institute for Applied Mechanics, Kyushu University, Kasuga, Fukuoka, Japan.
[4]Faculty of Education, Kagoshima University, Kagoshima, Japan.
[5]Institute of Low Temperature Science, Hokkaido University, Sapporo, Hokkaido, Japan.
[6]Solar-Terrestrial Environment Laboratory, Nagoya University, Chikusa, Nagoya, Aichi, Japan.
[7]Faculty of Environmental Studies, Nagasaki University, Nagasaki, Japan.
[8]Department of Earth Sciences, Seoul National University, Seoul, Korea.
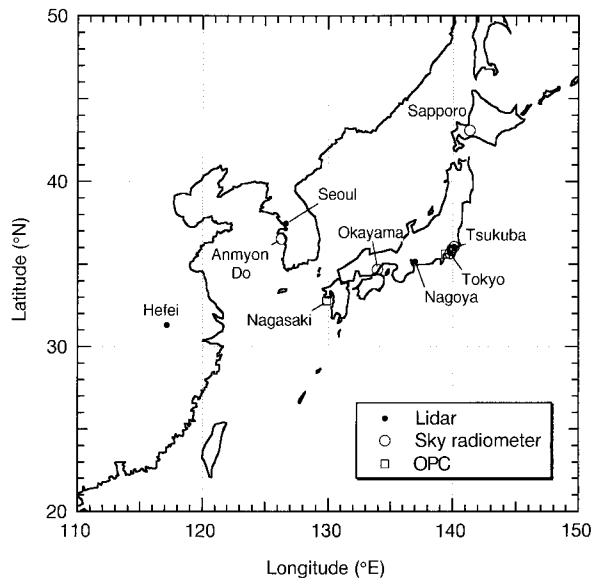[9]Department of Atmospheric Sciences, Seoul National University, Seoul, Korea.
[10]Anhui Institute of Optics and Fine Mechanics, Hefei, Anhui, China.
[11]Graduate School of Electrical Engineering, Tokyo Metropolitan University, Tokyo, Japan.
[12]Faculty of Engineering, Okayama University, Okayama, Japan.

meteorological concern in east Asia. The transport mechanism and the optical properties of Asian dust have been studied using ground-based instruments such as lidar, a Sun photometer, sky radiometer, and an optical particle counter (OPC) in the last two decades [*Iwasaka et al.*, 1983; *Kai et al.*, 1988; *Nakajima et al.*, 1989; *Tanaka et al.*, 1989; *Jinhuan and Jinhui*, 1994]. Since the dust particles have distinguishable physical and optical properties, including a yellow color (UV absorbing), large size, and nonsphericity, it is relatively easy to obtain the signature of Asian dust using ground-based instruments such as lidar and sky radiometers.

Asian dust rising from the dust storms that occur in the arid regions at high altitudes (1 to 2 km or more) in China and Mongolia is easily delivered into the free troposphere during the spring by the westerlies. It travels a long distance and sometimes reaches North America beyond the Pacific, as in April 1998. Satellite remote sensors such as the Sea-viewing Wide Field-of-view Sensor (SeaWiFS) and the Total Ozone Mapping Spectrometer (TOMS) revealed daily images of this traveling Asian dust plume [*Husar et al.*, this issue]. Mineral dust plays an important role from a climate study point of view, as do anthropogenic aerosols, especially when we consider the global trend of desertification caused by land development [*Sokolik and Toon*, 1996; *Tegen et al.*, 1996]. Asian dust has a significant effect on the atmospheric radiation budget because of the large emission amount [*Uematsu et al.*, 1983; *Iwasaka et al.*, 1983]. Thus a systematic study of Asian dust is required to clarify the optical properties related to climate forcing.

Figure 1. Location of ground-based observation sites.

Figure 2. Meteorological information during the dust episode of April 1998. The numbers indicate the dates of the dust storm occurrences at the observatories (solid circles). The solid line shows the pass of the cutoff low marked every 12 hours at 500 hPa. The dashed circles roughly represent the Takla Makan and Gobi deserts.

A number of ground-based lidars have been operated recently in the East Asia region. It is consequently possible to form a network to observe the vertical profiles of aerosols at multiple locations. This lidar network should provide useful information for studying the transport mechanism of tropospheric aerosols, particularly when combined with the satellite remote sensing data. The combination of a lidar and a sky radiometer and/or a Sun photometer should give complementary and thus quantitative information about the radiative characteristics of aerosols in clear daytime. We have been exchanging information through the Internet (e-mail and World Wide Web) during the spring since 1997 from ground-based observations of Asian dust events by lidars, Sun photometers, sky radiometers, and optical particle counters (OPCs) [*Murayama et al.*, 1998]. This seasonal campaign in Japan is currently named LINK-J (Lidar Network for Kosa observation in Japan). Figure 1 shows the observation sites of the lidars, sky radiometers, and OPCs in Japan, Korea, and China which are described in this paper. Some lidars and sky radiometers observed the same events during the large Asian dust event in April 1998. The recent development of transport models and computer resources enables us to simulate how the dust is emitted into the atmosphere and transported. The transport models are effective for understanding the phenomenon over a wide coverage area and for estimating the quantitative amounts, e.g., total emission of dust, while the experimental data are indispensable for validation and for some calibrations to improve the accuracy of the model.

In this paper we describe the results of ground-based observations in east Asia by lidars, sky radiometers, and OPCs during Asian dust events in April 1998. We also discuss the data of suspended particulate matter (SPM or PM_{10}, defined in section 3.3) and the dust images derived from NOAA/AVHRR. We compare the results of the observations with the transport model.

2. Meteorological Condition

Huge dust storms successively occurred in the mid-April 1998, caused by frontal activity on the Asian continent [*Husar et al.*, this issue]. The dates of dust storm occurrences at the meteorological stations near the source region are provided in Figure 2. These were read from the weather message (SYNOP); information near the Takla Makan desert region is apparently lacking.
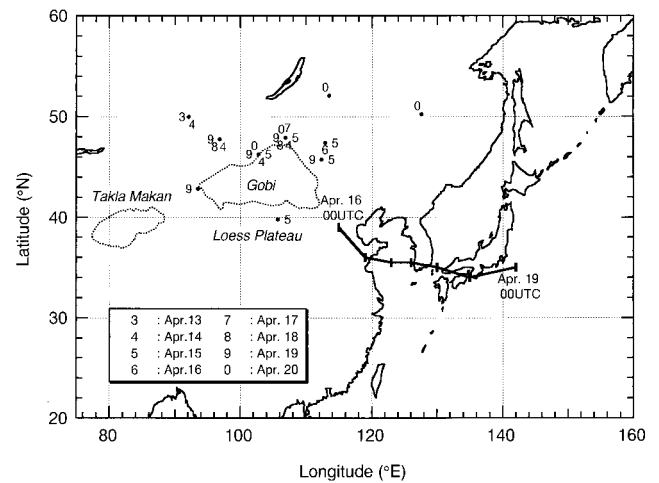
Tanaka [1998] described the relation between the cutoff low (or cutoff cyclone) and the Asian dust during this event using the visible satellite image of GMS 5. The cutoff low generated over the west of Beijing, which had a cold air mass at −23°C at 500 hPa on April 16, 1998, moved southwestward, accompanied behind by Asian dust. One feature of a cutoff low is its slow traveling speed. The movement of the cutoff low read from the weather map at 500 hPa is indicated in Figure 2. The cutoff low brought hail to the west of Japan. It disappeared over the Pacific to the east of Japan on April 19, 1998. A general description of a cutoff low is given by *Palmén* [1951] and *Ogura* [1993].

As described in section 4.2, not only the cutoff low but also the cold front that crossed over Japan brought Asian dust. Asian dust was observed widely in Japan under a high-pressure system after the passage of the traveling low. This pattern, i.e., Asian dust behind a cold front, is often observed for Asian dust events [*Kai et al.*, 1988; *Tanaka et al.*, 1989].

3. Ground-Based Observations in East Asia

The importance of international cooperation is increasing in aerosol studies as demonstrated by the Aerosol Characterization Experiment (ACE) [*Bates et al.*, 1998]. Since Asian dust is a typical aerosol in the free troposphere in the east Asia region and a matter of concern to several countries, it is an important subject for international cooperative studies. We exchanged information on Asian dust among our observation sites for the present study. One of the authors, J. Zhou, in Hefei, China, related the occurrence of severe dust storm events on April 17, 1998. This announcement triggered observations at Japanese sites in advance of the appearance of Asian dust over Japan. Thus information from regions near the source is very impor-

Table 1. Ground-Based Observation Sites and Instruments

| Site	Institute	Latitude, Longitude, msl	Instruments
Hefei	AIOFM.	31.31°N, 117.16°E, 31m	lidar
Seoul	SNU.	37.46°N, 126.65°E, 150m	lidar
Anmyon Do	SNU.	36.52°N, 126.32°E, 47m	sky radiometer
Nagasaki	Nagasaki Univ.	32.78°N, 129.87°E, 16m	OPC
Okayama	Okayama Univ.	34.68°N, 133.95°E, 7m	sky radiometer
Nagoya	Nagoya Univ.	35.15°N, 136.97°E, 75m	lidar
Tokyo	TUMM	35.66°N, 139.80°E, 3m	lidar, sky radiometer
	TMU	35.62°N, 139.38°E, 135m	OPC
Tsukuba	NIES	36.05°N, 140.12°E, 23m	lidar, sky radiometer
Sapporo	Hokkaido Univ.	43.08°N, 141.34°E, 15m	sky radiometer

tant for network observations, unless the instruments are continuously operated in unattended mode. The Asian dust event continued for an extraordinarily long period in Japan from April 18 to 23. In this section we present the data obtained by the lidars, sky radiometers, and the OPCs in China, Korea, and Japan. The location of the sites and the corresponding instruments are listed in Table 1. There is no time difference between Korea and Japan; the LT is nine hours in advance of UTC in those counties, while the LT in China is eight hours in advance of UTC.

3.1. Observation by Lidar

The setup and performances of the lidar systems in the network observation differed depending on the site, because the lidars had been prepared by the participating organizations separately for their own purposes. A common feature of the lidars is the laser wavelengths which are generated by Nd:YAG lasers (355, 532, and 1064 nm) or Nd:YLF lasers (523 nm). The details of each lidar system and the data analysis method are presented in the references cited below. In this paper we report the observation results at each site with a visible laser wavelength (532 or 523 nm).

3.1.1. In China.
Lidar observations of the stratospheric and tropospheric aerosols have been carried out routinely at the Anhui Institute of Optics and Fine Mechanics (AIOFM), located 15 km west of Hefei [*Hu et al.*, 1998; *Zhou*, 1998]. The "L300 lidar" was operated during the Asian dust events of April 16 and 18, 1998. The observation wavelength was 532 nm. Profiles of the extinction coefficient were derived with Fernald's method [*Fernald*, 1984]. The boundary condition was given near the tropopause, and an extinction to backscatter ratio (the lidar ratio S_1, as defined later) of 50 was used [*Zhou*, 1998]. The vertical extinction profiles obtained on April 16 and 18, 1998, are shown in Figure 3 with both linear and logarithmic scales. The vertical resolution is 30 m. The dust layer was mainly concentrated in the troposphere lower than 5 km in altitude, and the extinction coefficient reached 0.5 km^{-1} or more near ground level. A floating layer that peaked around 3 km was commonly seen. Another feature was the presence of a thin dust layer in the higher troposphere (6 to 10 km), which
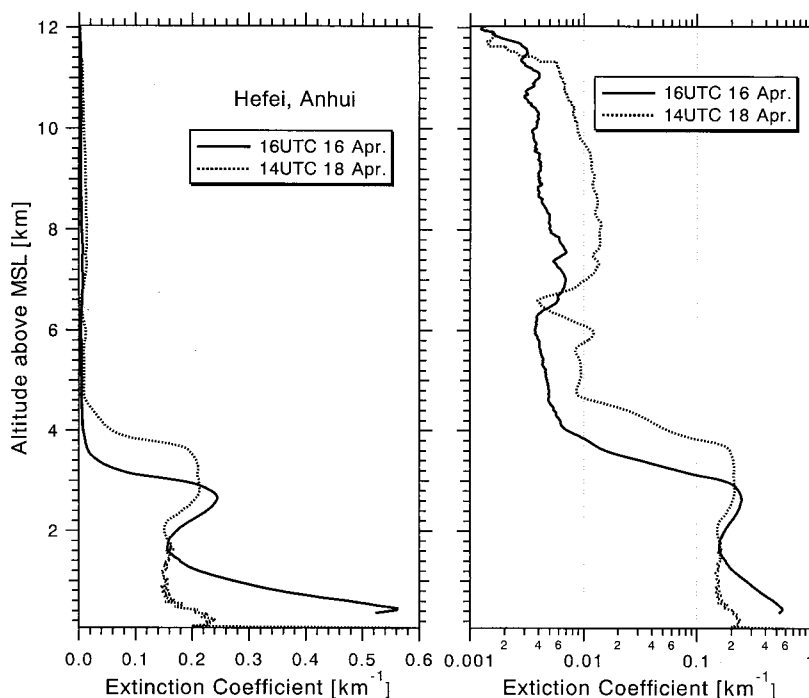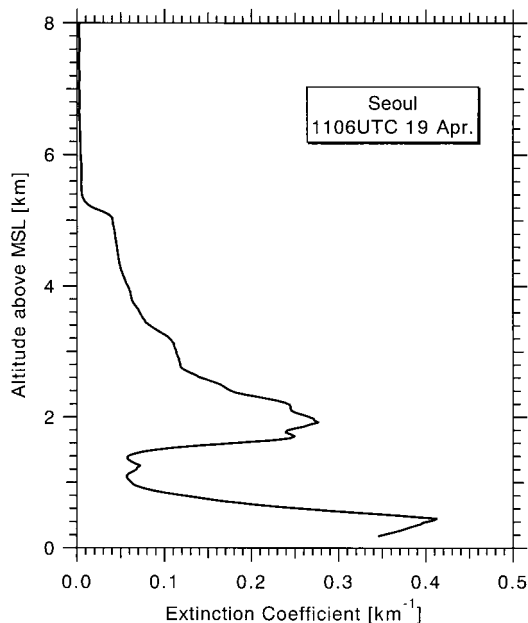

Figure 3. Vertical profiles of aerosol extinction coefficient in linear and logarithmic scales on April 16 and 18, 1998, over Hefei, China.
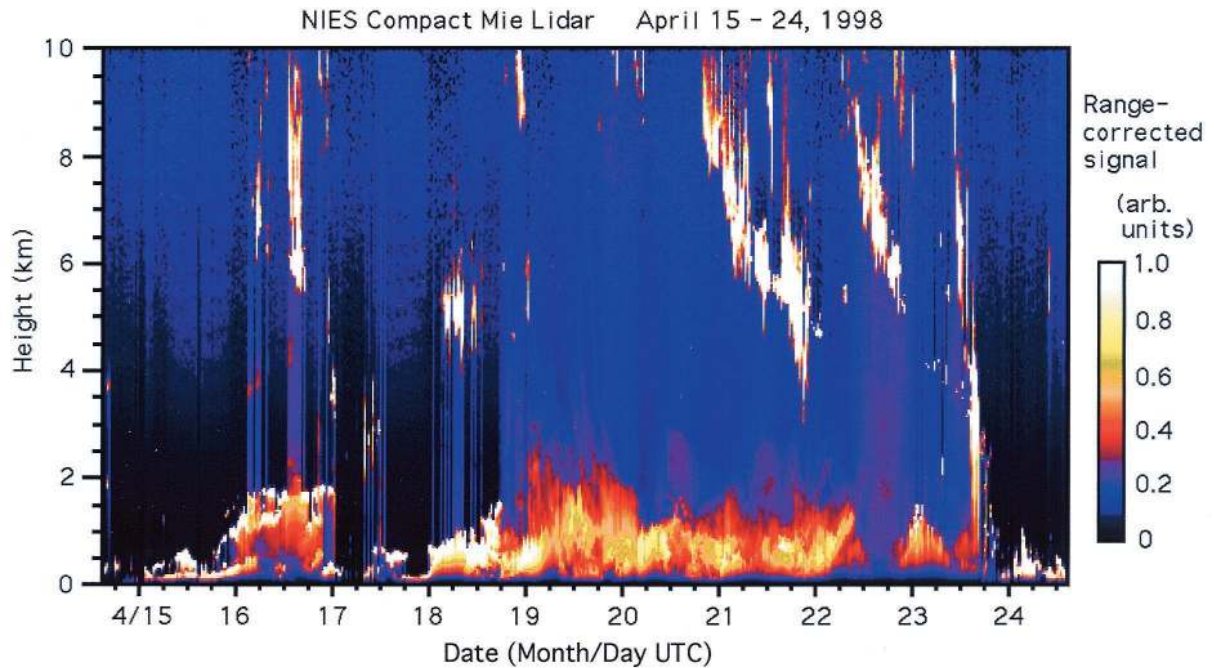
Plate 1. Time-to-height indication (THI) of the range-corrected backscattering intensity (in arbitrary units) obtained by the CML of NIES in Tsukuba during April 15 to 25, 1998. The signals from clouds (white regions) often exceeded the upper scale.
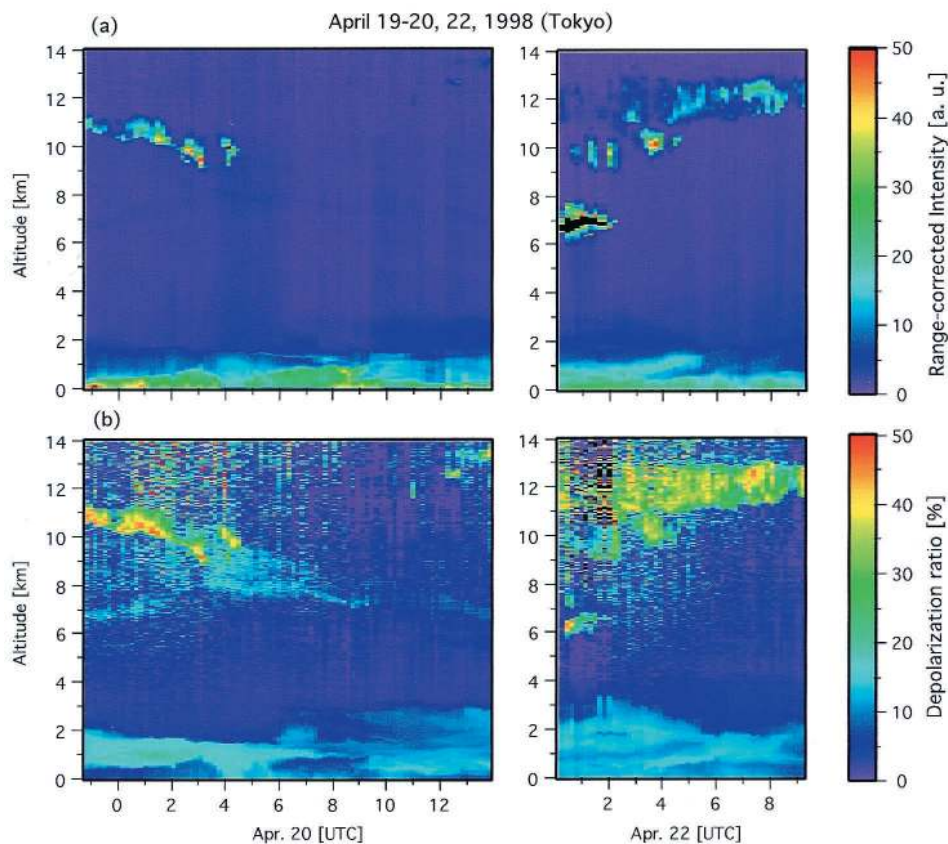
Plate 2. THI of the range-corrected backscattering intensity and the depolarization ratio on April 19–20 and 22, 1998, obtained at TUMM in Tokyo. (a) Range-corrected backscattering intensity, (b) depolarization ratio. The black portion gives the values that exceeded the maximum of the scale.

Figure 4. Vertical profile of the aerosol extinction coefficient on April 19, 1998, over Seoul, Korea.

had an extinction coefficient peak of the order of 0.01 km^{-1}. This feature will be discussed in section 5.3.

3.1.2. In Korea. Seoul National University (SNU) in Seoul has routinely operated a micropulse lidar (MPL) to monitor the troposphere [*Yoon and Won*, 1998]. The MPL is a commercial lidar developed by *Spinhirne* [1995] and manufactured by SES Inc. (Maryland, United States) [*Lee et al.*, 1997]. The emitting laser wavelength is 523 nm generated from a Nd:YLF laser. The MPL was continuously operated during the period of April 18 to 20, 1998, and the Asian dust plume was observed [*Yoon et al.*, 1999]. Details of the analytical procedure used to derive the extinction coefficient profiles from the MPL were described by *Yoon and Won* [1998]. A typical vertical profile on April 19, 1998, is shown in Figure 4. The vertical resolution was 30 m. A floating dust layer with a peak around 2 km and that spread to 5 km is seen. This structure is similar to the lidar observation in Hefei.

3.1.3. In Japan. Several lidars were operated during the Asian dust event in Japan, including a polarization lidar (532 nm) from Okayama University in Okayama (the preliminary results of the Okayama lidar were presented in a previous report [*Murayama et al.*, 1998]), a Raman lidar (355, 532, 1064 nm) from the Solar Terrestrial Environmental (STE) Laboratory of Nagoya University in Nagoya [*Shibata et al.*, 1996], a polarization lidar (532 nm) from Tokyo University of Mercantile Marine in Tokyo (TUMM) [*Murayama et al.*, 1999a], and a compact Mie lidar (532 nm)) [*Matsui and Sugimoto*, 1997] and high spectral resolution lidar (HSRL, 532 nm) [*Liu et al.*, 1999] from the National Institute of Environmental Studies (NIES) in Tsukuba. A polarization lidar is a Mie-scattering lidar that can measure the polarization properties of backscattering. It is useful detecting ice phases in clouds [*Sassen*, 1999] and also for detecting a dust layer [*Kobayashi et al.*, 1985; *Murayama et al.*, 1998] since the cross-polarized component is sensitive to the nonsphericity of the scatter. A Raman lidar can obtain the water vapor mixing ratio and aerosol optical properties; water vapor can have a significant effect on the optical properties and

the evolution of aerosols [*Ansmann et al.*, 1992; *Whiteman et al.*, 1992; *Sakai et al.*, 2000]. A HSRL can separately measure the Mie and Rayleigh backscattering components and thus yield backscattering and extinction coefficients without the assumption that is necessary for a conventional Mie lidar analysis [*Shipley et al.*, 1983]. We will first describe some continuous lidar observations of the dust episode and then report on simultaneous observations in Japan.

The compact Mie lidar (CML) at NIES has been operated in a continuous mode (5 min of data acquisition with 10-min intermissions) through an equipped window on the roof of the lidar container, which enables continuous measurement without dependence on weather conditions. The data obtained are very useful as a comparison with the model prediction since there is no interruption of data. Plate 1 shows the time to height indication (THI) of the range-corrected lidar signal, i.e., the attenuated backscattering intensity, including the Mie and Rayleigh components, obtained by the CML during the Asian dust episode. The overlapping between the field of view of the receiver and the laser beam (called the overlapping function) is not complete below a height of about 400 m. The vertical recording resolution is 7.5 m. The range-corrected backscattering in arbitrary units does not have a clear physical meaning. However, it is useful to see the full vertical structure of the troposphere, including aerosols and clouds, the optical properties of which are so different that it is difficult to treat them in a uniform way. The CML and HRSL at NIES observed the leading edge of the aerosol layer at an altitude of about 6 km around 1300 UTC, April 19, 1998. The high concentration of aerosols was thereafter continuously observed below 3 km until April 23, 1998.

TUMM polarization lidar was operated continuously in Tokyo on April 20 and 22, 1998. The lidar has two polarization-diverse telescopes to expand the dynamic range of detection; one is dedicated to short-range detection and the other to long-range. The overlapping function of the lidar became unity above 150 m in height in the measurements, and the depolarization ratio was usable above 27 m in height. The data acquisition time for one profile was 10 min. Plate 2 shows the THIs of the range-corrected backscatter intensity and the depolarization ratio. The vertical resolution of the record was 6 m but was reduced to 18 m above 2 km to improve the signal-to-noise ratio. Here we define the depolarization ratio as the ratio of the backscattered signals of the perpendicular to the parallel polarization of backscattered lights with the emitted linear polarized laser. These data reveal a higher depolarization ratio than usual (normally less than several percent) in the lower troposphere [*Murayama et al.*, 1996], and the dust was mostly below 3 km during the dust episode. Another striking feature seen in Plate 2 is the complete negative correlation between the backscattering intensity and the depolarization ratio below 2 km, where the dust mixed with boundary layer (urban) aerosols. This feature was interpreted by the external mixture of the dust with the anthropogenic aerosols. A detailed explanation will be provided elsewhere.

Simultaneous lidar measurements were performed at Nagoya (STE), Tokyo (TUMM), and Tsukuba (NIES) around 1230 UTC, April 20, 1998. The scattering ratio, depolarization ratio, and relative humidity are shown in Figure 5 with the radiosonde data obtained at Tateno (Tsukuba) at 1200 UTC. The scattering ratio $R(z)$ at the altitude z is defined as

$$R(z) = [\beta_1(z) + \beta_2(z)]/\beta_2(z), \qquad (1)$$
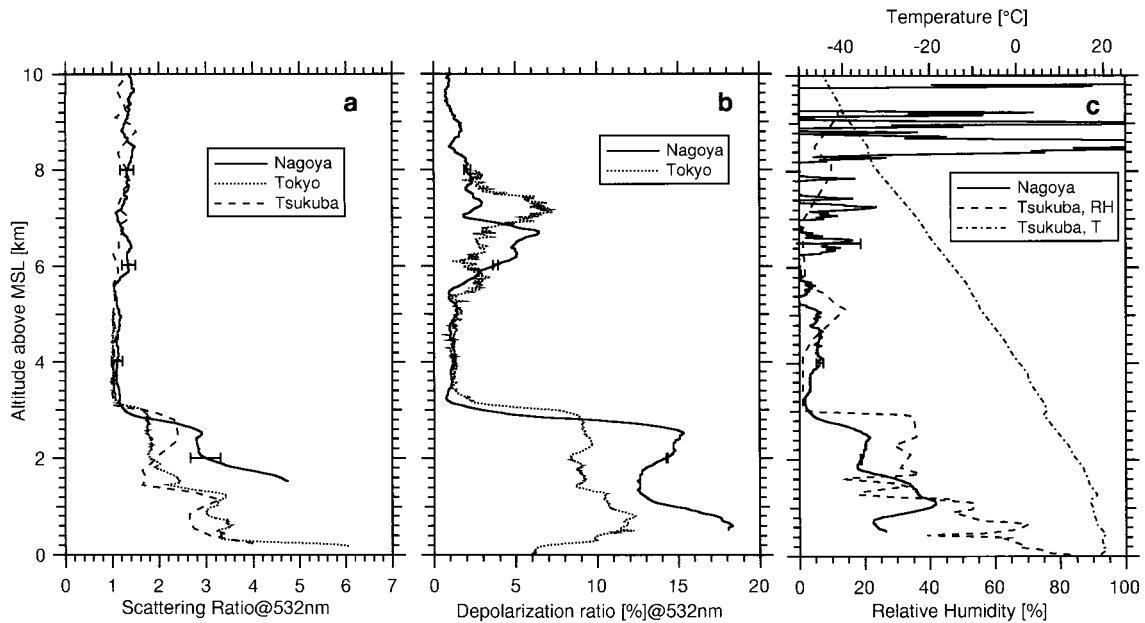
Figure 5. Simultaneous lidar observations at Nagoya, Tokyo, and Tsukuba around 1230 UTC April 20, 1998. (a) Scattering ratio at 532 nm, (b) depolarization ratio at 532 nm, and (c) relative humidity. The measurement durations were 1233 to 1303, 1228 to 1309, and 1205 to 1305 in UTC for Nagoyo, Tokyo, and Tsukuba. Temperature and relative humidity profiles by radiosonde observation at Tateno (Tsukuba) are also indicated in Figure 5c.

where β_1 and β_2 are the backscattering coefficients by aerosols (subscript 1) and air molecules (subscript 2). The extinction coefficient of aerosol σ_1 is converted to the backscattering coefficient of aerosols with the lidar ratio S_1, i.e., $\sigma_1 = \beta_1 \cdot S_1$. However, S_2 ($= \sigma_2/\beta_2$) for the air-molecule scattering is known as $8\pi/3$ from the Rayleigh-scattering theory. The backscattering coefficient β_2 is evaluated from the air density profiles given by the atmospheric model or the radiosonde data. The vertical resolution of the HSRL was 150 m. The data of the STE Raman lidar had a vertical resolution of 330 m, which was smoothed by taking the running mean of the recorded 30-m resolution data to improve the signal-to-noise ratio. The scattering ratio at TUMM was obtained by Fernald's method with the atmospheric density evaluated from the radiosonde data. Here we assumed the $R(z)$ to be 1.05 at $z = 6$ km as the boundary condition, and the extinction coefficient was solved downward with a uniform lidar ratio S_1 of 45. In the depolarization ratio at TUMM shown in Figure 5b, 1% was subtracted from the raw value to correct the expected offset [*Murayama et al.*, 1999a].

The dust heights obtained by these data were below 3 km, which corresponds to the temperature inversion (Figure 5c). The dust concentration in Nagoya should have been somewhat higher than in the Tokyo region, as indicated by the scattering ratio and depolarization ratio. The humidity obtained by Raman lidar shows the proportional behavior of the scattering ratio in this layer. A thin but high depolarizing layer lay between 5.5 and 8.0 km in altitude, which was considered to be a thin dust layer and not ice crystals because the relative humidity was less than 30%. This is also supported by the moderate temporal behavior of lidar backscattering from this layer observed in Tokyo (Plate 2). We will discuss the role of this high-altitude thin dust layer in section 5.2.

3.2. Observation by Sky Radiometer

We used a common sky radiometer in addition to the lidar; the procedure of the data analysis is described below. The sky radiometer was designed by *Nakajima et al.* [1996] and manufactured by Prede Co. Ltd. (Tokyo, Japan, model POM-01). The apparatus can measure direct and diffused solar radiation in almucantar mode at several observation wavelengths, e.g., 315, 400, 500, 675, 870, 940, and 1020 nm. The 315 and 940 nm channels are designed to retrieve the column contents of ozone and water vapor, respectively. The other channels are used for retrieval of the aerosols. We performed a unified analysis of the sky radiometer data using a program developed by *Nakajima et al.* [1996]. It is known that the optical thickness and size distribution of aerosols are relatively insensitive to the refractive index used in the present analysis and that the forward scattering is not sensitive to the nonsphericity of the particles [*Pollack and Cuzzi*, 1980]. Therefore we used normalized radiance data from 4° to 30° in scattering angle for the inversion and a fixed refractive index $m = 1.55 - 0.01i$ as the input parameter, which is often used for dust-like aerosols [*Nakajima et al.*, 1989]. We used a ground albedo of 0.1 for all the channels as the input parameter. The locations of the sky radiometer sites are shown in Figure 1. The sky radiometer was installed at the background-monitoring site in Anmyon Do in Korea, which is an island located off the west coast of the Korean peninsula. In Japan, we used the data obtained at Sapporo, Tsukuba, Tokyo, and Okayama.

Figure 6 shows the derived aerosol optical thickness (AOT) at 500 nm and the Angström exponent (α) after fitting the empirical formula [*Angström*, 1961] for the AOTs at all the observation wavelengths during the dust episode. We can clearly see the indication of Asian dust events at all sites; the
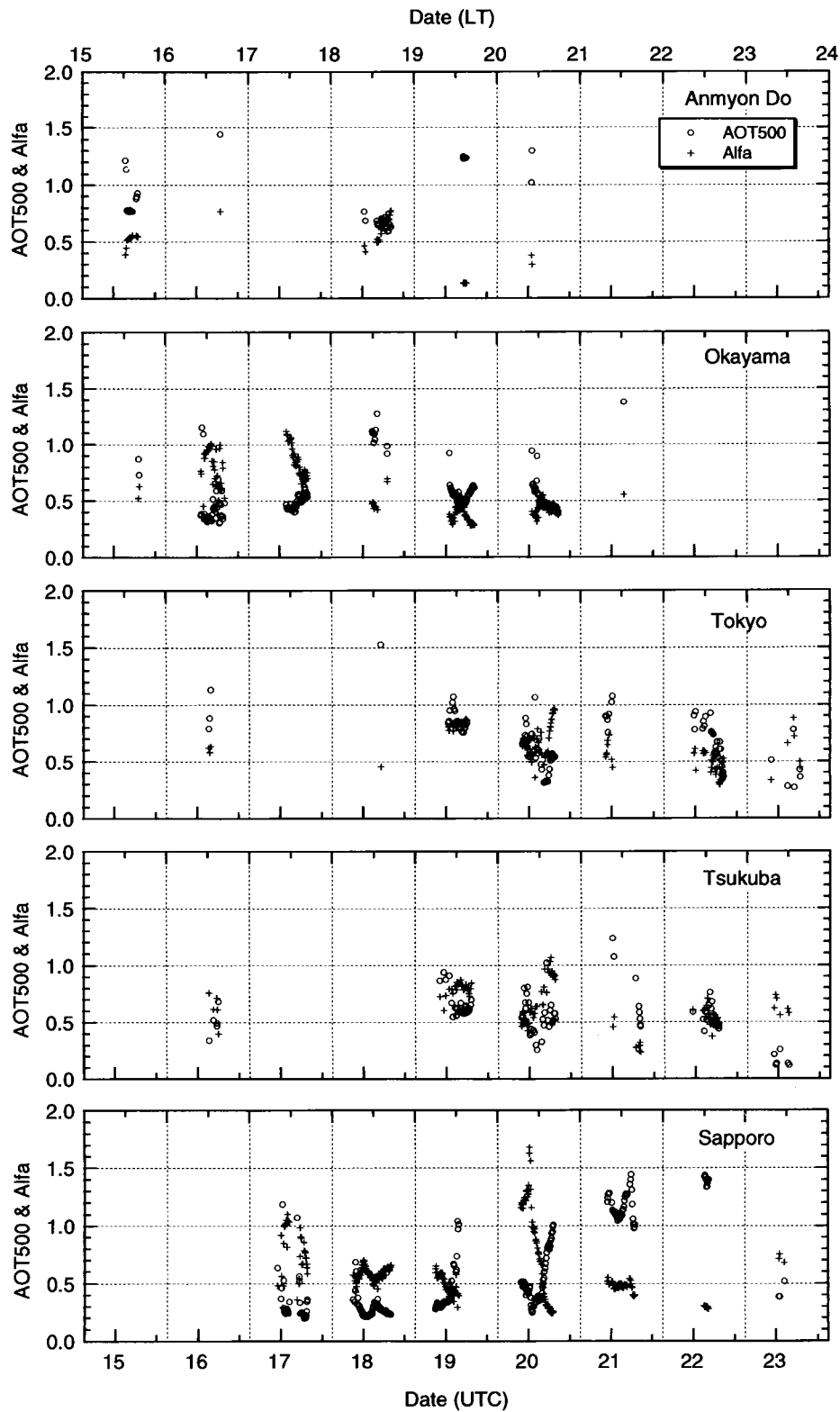
Figure 6. Aerosol optical thickness at 500 nm (AOT500) and the Angström exponent (Alfa) derived from the sky radiometers from April 15 to 23, 1998, in Korea and Japan.

Angström exponent became lower than the usual value of 1.5. For example, the rapid increase of Asian dust in the air column, as indicated by a low α and high AOT, is clearly seen in the Sapporo data on April 20. Figure 7 shows the retrieved volume size distributions in the air columns for representative cases. We can see that the coarse mode radius commonly locates around 2 μm. This result is consistent with previous reports on the size of Asian dust in Japan [*Arao and Ishizaka*,
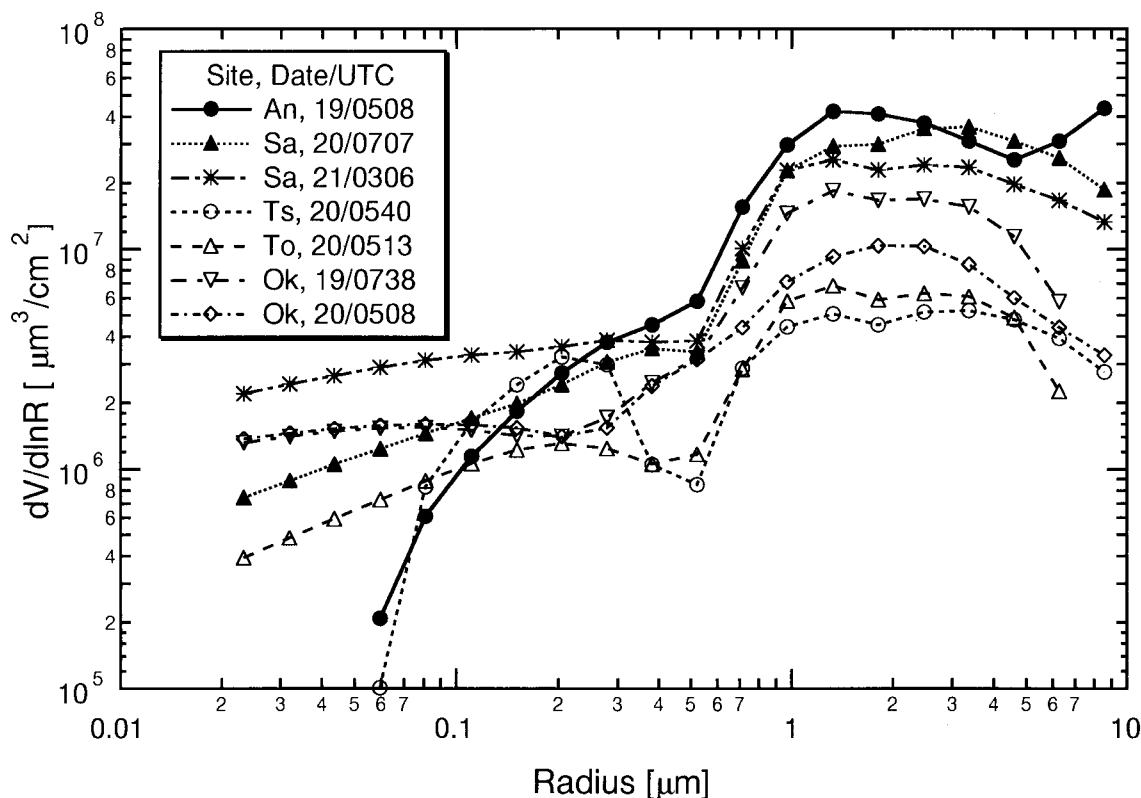
Figure 7. Representative volume size distributions retrieved from the sky radiometers in Anmyon Do (An), Sapporo (Sa), Tsukuba (Ts), Tokyo (To), and Okayama (Ok) during the dust episode of April 1998.

1986; *Tanaka et al.*, 1989]. Thus the sky radiometer is very useful for detecting Asian dust events, as is the polarization lidar, although the data are limited in clear daytime.

### 3.3. Observation by an Optical Particle Counter and Other Devices

We also used an OPC to detect the Asian dust events. Since large particles more than 5 μm in diameter are few under the usual conditions, it can be used as an index of Asian dust on the surface. Here we present the data obtained by the OPCs manufactured by Rion Co., Ltd. (Tokyo, Japan); models KC-01B and KM-07C were used in Nagasaki and Tokyo (Tokyo Metropolitan University (TMU)), respectively. These OPCs have five or two channels according to the discriminating diameters. The sampling speed of the air was 0.5 and 2.83 L/min. The OPCs were calibrated by the manufacturer with monodisperse polystyrene latex aerosol with a refractive index of $m = 1.595 - 0.0i$. In this paper we present particle count data larger than 5 μm in diameter. We also used the PM_{10} records obtained at the air pollution monitoring stations in Fukuoka and Tokyo for a comparison with the results of the model. Suspended Particulate Matter (SPM, called PM_{10}) is defined in the ambient air quality standard in Japan as the mass of aerosols sampled through a 10-μm-cut size separator. The PM_{10} was measured at the stations every hour with beta-ray absorption-type automated monitors; the measurement resolution was about ± 10 μg/m^3. The particle counts larger than 5 μm per unit volume at Nagasaki and the PM_{10} concentration at Itoshima in Fukuoka, which is a rural site located about 100 km north-northeast of Nagasaki, are shown in Figure 8. We can see the passage of the dense dust clouds from April 17 to 18,

1998, indicated by shape peaks in both the OPC and the PM_{10}. These OPC records are the highest of the previous several years in Nagasaki [*Arao and Sakaguchi*, 1999]. The OPC data at TMU (about 45 km west of TUMM) and the PM_{10} data near TUMM in Tokyo are given in Figure 9. Note that the scale of the OPC data in Nagasaki is 10 times larger than that in Tokyo. The PM_{10} data in Fukuoka must be more sensitive to the Asian-dust loading than in Tokyo, because high local aerosol emissions in urban areas tend to hinder the Asian dust contribution. Nevertheless, we can clearly see the greater than usual PM_{10} even in Tokyo during the Asian dust episode. The time lag of the dust episode between the Kyushu region (Fukuoka and Nagasaki) and Tokyo was about 1 to 2 days. The lidar and sky radiometer data indicate that the dust partly covered the Tokyo region on April 19, but the OPC in Figure 9b shows that more dust had arrived on the surface on April 20. Such time lag is often observed at the beginning of an Asian dust event [*Murayama et al.*, 1999b]. Furthermore, we can clearly see a diurnal pattern in the dust concentration in the OPC data; the concentration increased in the daytime. This might be due to the diurnal cycle of the entrainment process between the free troposphere and the boundary layer [*Husar et al.*, this issue].

4. Comparison of Observation Results With the Transport Model

In this section we will describe the outline of the tracer model of the dust and the comparison of our simulation results with the observations, including the satellite remote sensing. We also discuss the results of conventional trajectory analysis.
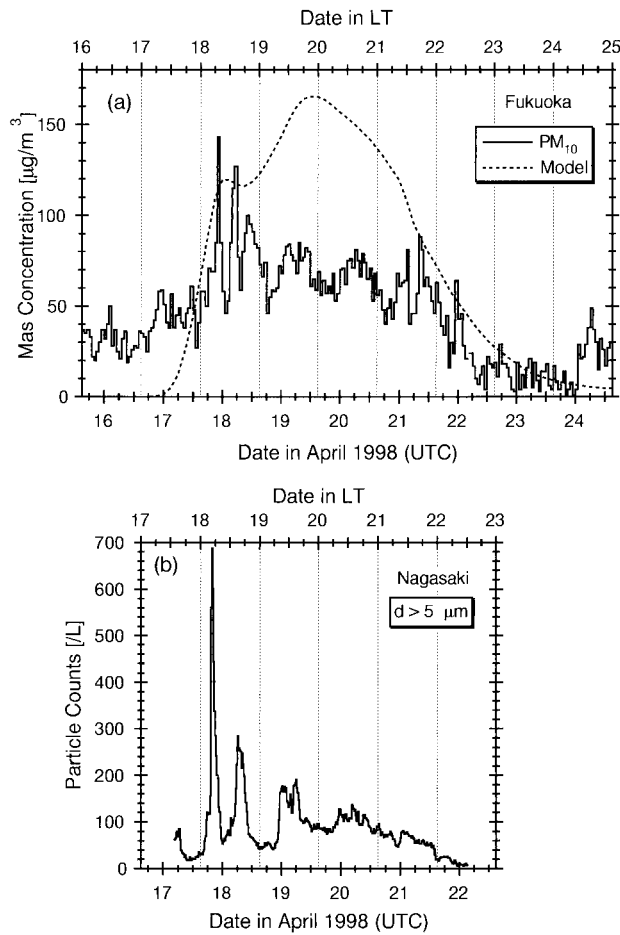
Figure 8. (a) PM$_{10}$ at Fukuoka. (b) The particle counts larger than 5 μm in diameter per liter measured by the OPC at Nagasaki during the dust episode of April 1998. The dust concentrations every 3 hours simulated by the model (dashed curve) are superposed in Figure 8a.
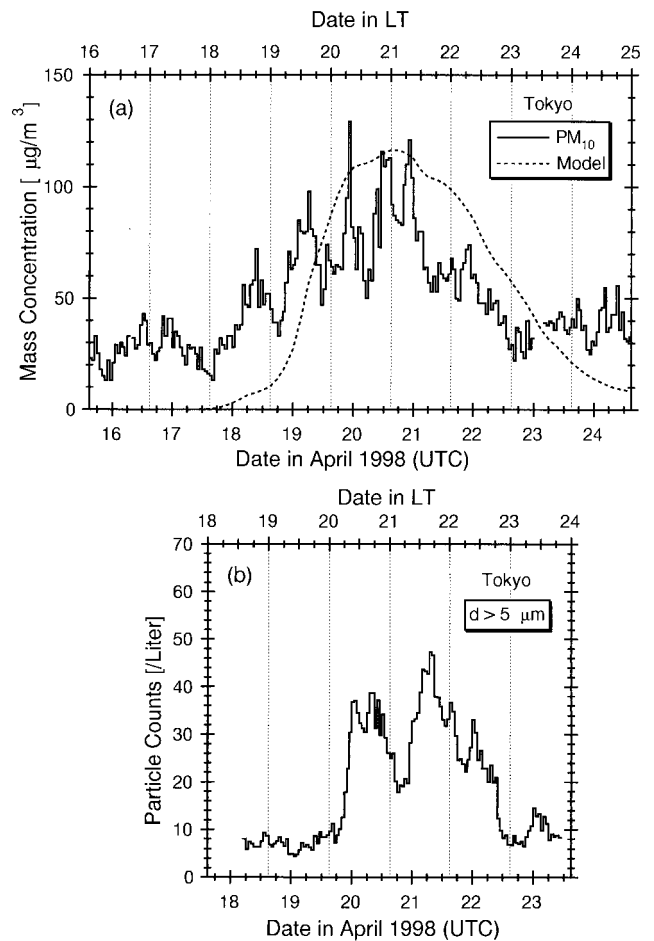
Figure 9. Same as in Figure 8 except the locations. (a) The PM$_{10}$ at Koto (near TUMM) in Tokyo and the simulation (dashed curve). (b) The particle counts larger than 5 μm in diameter per liter by the OPC at TMU in Tokyo.

4.1. Outline of the Model

An on-line tracer model coupled with a Regional Atmospheric Modeling System (CSU-RAMS) [*Pielke et al.*, 1992] was developed to study the natural dust and trace gas transport. The tracer model was strongly coupled with a comprehensive meteorological model, since regional meteorological conditions such as precipitation, cloud microphysics, and the diurnal cycle of boundary layer turbulence play significant roles in the advection and diffusion of tracers. The on-line tracer model was built into the RAMS, and it ran with the same time step as the RAMS. The dust emission area was the area where the Matthews vegetation type [*Matthews*, 1983] is assigned to the desert. Most of the Gobi and Takla Makan deserts are indexed as source regions.

We used the dust roll-up scheme proposed by *Gillette* [1978]; that is, the dust mass loading F_{dust} is defined by

$$F_{\text{dust}} = C(U - U_{tr})U^2, \qquad (2)$$

where C is the emission constant, U is the surface wind speed, and U_{tr} is the critical wind speed of the dust roll-up ($U_{tr} = 6.5$ m/s was used in this study, and $F_{\text{dust}} = 0$ if $U < U_{tr}$). The dust lift-up height (mixed layer) was determined from the vertical profile of the potential temperature. The RAMS built-in hor-

izontal and vertical advection and turbulent diffusion scheme were used for the dust. The dust dry deposition velocity v_g was determined to be $v_g = C_D U_{10}$, where C_D is the bulk-transfer coefficient derived from the RAMS surface-layer scheme, and U_{10} is the wind speed at a 10 m height. A simple dust washout scheme as a function of the surface precipitation rate was also included in the transport model study.

The model study was conducted for the period from April 13 to 30, 1998, using four-dimensional data assimilation (4DDA) based on ECMWF global analysis data. A model domain covering all of the China-Korea-Japan area was designed by a polarstereographics coordinated system (centered at 110°E, 40°N; horizontal grid spacing of 120 km and 60 × 56 grid system). The model top was placed at 18 km with a 23 vertical grids system.

### 4.2. Comparison Between NOAA/AVHRR Image and Model Calculation

Satellite images are useful for studying the horizontal extension of Asian dust over land and sea, together with the lidar data, which is valuable for studying the vertical structure. During the Asian dust events in mid-April 1998, dense dust above the Chinese continent was seen in the visible-band images of the GMS-5/VISSR [*Murayama et al.*, 1998] and SeaWiFS as a
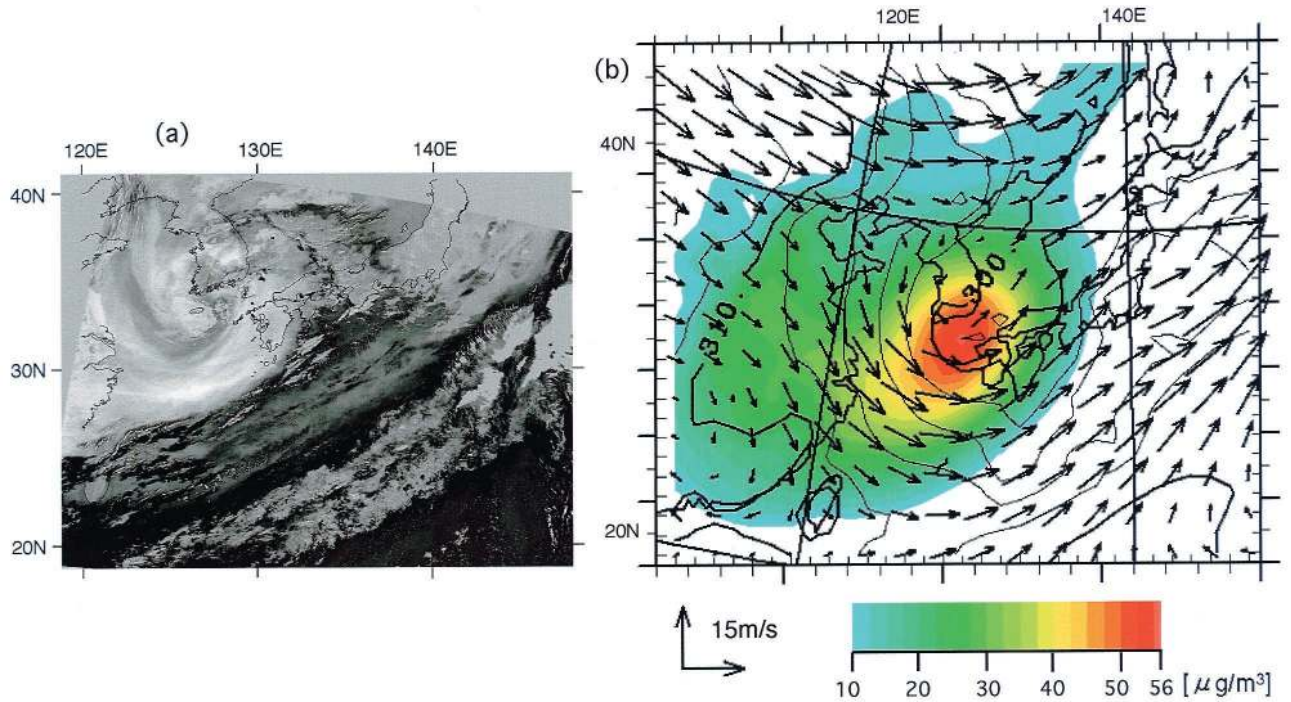
Plate 3. (a) AVI image of the brightness temperature difference at 1755 UTC, April 17, 1998. (b) The simulated column average concentration of dust, wind vector, and potential temperature at an altitude of 3000 m at 1800 UTC, April 17, 1998.
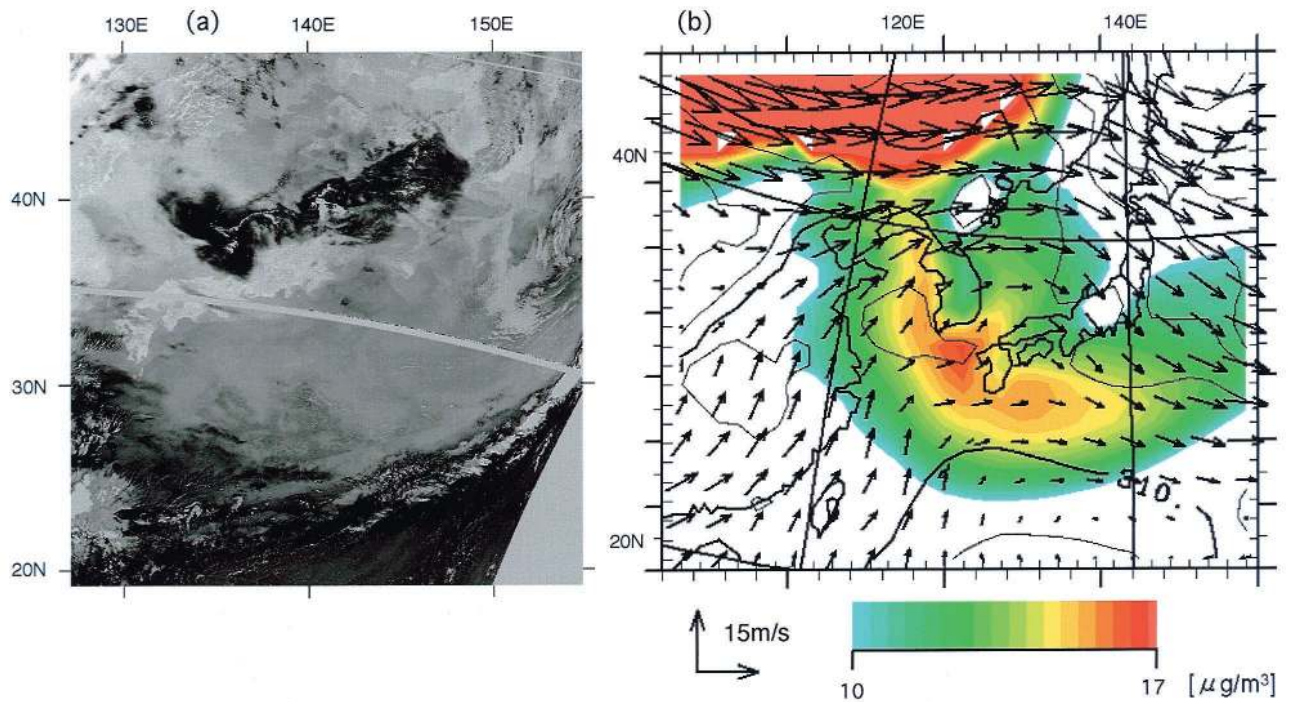
Plate 4. Same as Plate 3 except the time. (a) The AVI image at 1733 UTC, April 19, 1998. (b) The simulation at 1800 UTC, April 19, 1998. The red region at the left top corner of the simulated column average concentration exceeded the maximum scale.
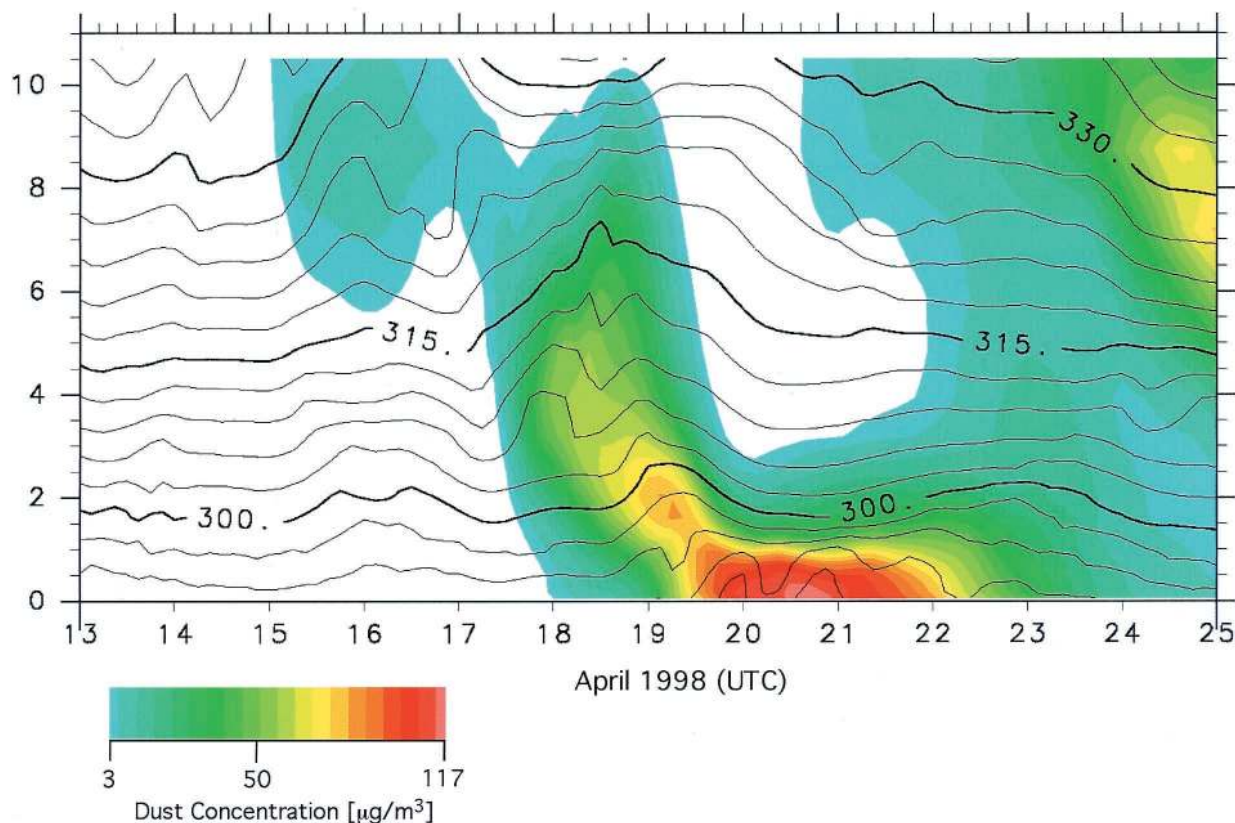
Plate 5. Time-to-height cross section of the dust concentration and the potential temperature (contour line) over Tokyo given by the model during the dust episode.

dust storm in a cloud-free area. Transportation of the dust toward the east, extending and diffusing with time over the Yellow Sea, Korea, and the Japanese Islands to the Pacific Ocean, was detected by means of the brightness temperature difference of AVHRR-4 and AVHRR-5 of the NOAA satellites [*Kinoshita et al.*, 1999].

The diffused Asian dust in the visible and near-infrared band images that reflected the solar radiation in daytime was generally rather vague with a weak signal [*Murayama*, 1988]. The SeaWiFS sensor provided improved information with higher sensitivity to the aerosol in shorter wavelengths, though careful distinction from the effect of the ocean color was required [*Fukushima et al.*, 1999]. In contrast, the split window method that shows the differences between the AVHRR-4 and AVHRR-5 channels (10.5 to 11.5 and 11.5 to 12.5 μm) was found to be very effective to detect the extension of the Asian dust aerosol with varying density in day and night. The split window method has been utilized to estimate the vapor amount to ascertain the sea surface temperature [*Inoue*, 1990]. There is an opposite emissivity difference of lithic dust and aerosol in the 11 and 12 μm bands against water vapor [*Takashima et al.*, 1987], and this is useful for detecting them [*Prata*, 1989; *Imasu*, 1992].

Plates 3a and 4a show two examples of the NOAA/AVHRR images of Asian dust around Japan. These are the brightness temperature differences of channels 4 and 5 in the form of the Aerosol Vapor Index (AVI), defined as AVI $= n(5) - n(4) + 200$, where a 10-bit value $n(i)$ of thermal infrared band i is related to the brightness temperature $t(i)$ in centigrade as $t(i) = -50 + 0.1n(i)$, for $i = 4$ and 5. The bright

parts in the gray scale images of the AVI correspond to high AVI domains with dense aerosol, while the dark parts show the domains of dense vapor above the opaque surface. Very bright domains with $t(4) \ll t(5)$ were seen above northern China and the Yellow Sea in the images on April 16, 1998 (not shown here), indicating very dense Asian dust aerosol. In the images from April 17 and 19, shown in Plates 3a and 4a, the Asian dust was somewhat diffused compared with previous days. However, its extension over Japan is clearly seen in both images; in Plate 3a, a bright dust domain is seen as a brush stroke sweeping over Kyushu Island in western Japan due to the cutoff low mentioned in section 2, while the Asian dust extends in Plate 4a over all of Japan and the Pacific Ocean up to the front line in the southeast corner, which separates the dust-free vapor-rich domain of oceanic atmosphere, as on 18 April (not shown here). The sequential changes of the Asian event in the AVI images on these days conform very well to the model calculations. Plates 3b and 4b show the calculated wind vector and potential temperature at altitude $z = 3000$ m and the dust column-averaged concentration (contour) for April 17 and 19, 1998, by the model. The cutoff low was observed behind this cold front (over the main China Plain), and its vortex trapped a huge amount of dust and moved slowly to the east.

4.3. Comparison With Ground-Based Observation

A very severe dust storm was observed on April 14 to 15, 1998, at Xinjian Province, China, and the satellite image clearly captured the onset of this dust front and dust cloud. The daily dust flux simulated in the model indicated that more than 50% of the total dust emission between April 13 and 23
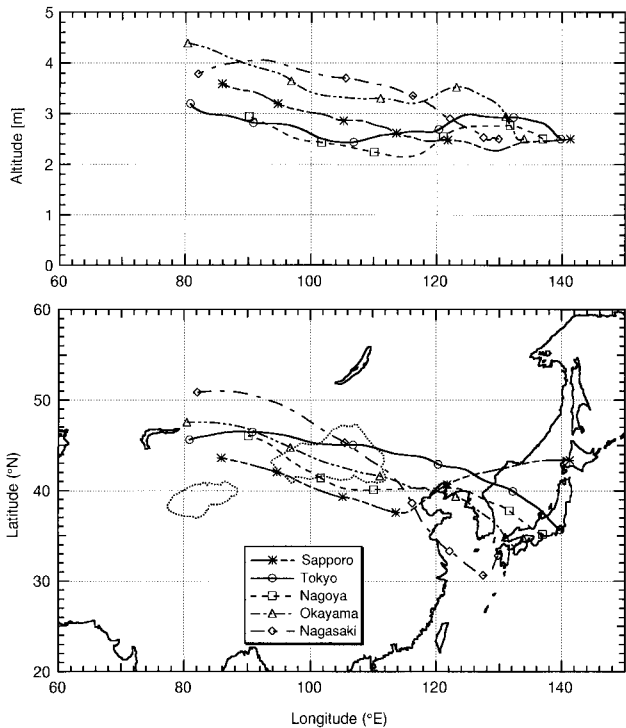
Figure 10. Results of the 5-day backward trajectory analysis started from an altitude of 2500 m over the Japanese observation sites at 1230 UTC, April 20, 1998. Symbols denote the location of the air mass every 24 hours.

occurred within the two days of April 14 and 15. The daily dust transport simulated by the on-line tracer model clearly revealed an eastward traveling strong low-pressure system and cold-frontal line was responsible for this strong dust episode. The model analysis also indicates that it took 3 days to travel from the foot of Shandong Peninsula to Tokyo, as mentioned in section 2, and this slow movement of the cutoff vortex agreed with the dust peak time lag observed at several Japanese observation sites.

The numerical results were compared with the lidar observations, ground-based PM_{10} observations, and the OPC data in Japan. The calculated surface dust concentrations at Fukuoka and Tokyo are given in Figures 8 and 9. The peaked concentration in Fukuoka and the time lag of the dust episode are reproduced. The sharply peaked dust concentration must have been formed by the vortex; there was a banded structure of dust concentration along the vortex. This tendency was also seen in the dust image obtained from NOAA/AVHRR (Plate 3a).

A time-to-height cross-section analysis, shown in Plate 5, indicated that (1) a dense dust layer existed at a height below 2 to 3 km (within the planetary boundary layer (PBL)), which agrees well with the lidar observations shown in Plates 1, 2, and Figure 5, and (2) the dust concentration correlated with the potential temperature variation. A strong descending motion and temperature subsidence on the west side of the cutoff vortex was responsible for the dust episodes in the southern parts of China and Japan. However, the effect seemed to be less in Tokyo because the vortex was getting weaker. A sensitivity analysis conducted by introducing the daily independent dust emission (i.e., the daily dust emission is treated as a

different tracer) indicated that the dust episode over Japan was brought by the dust emission on April 14 and 15.

4.4. Comparison With Trajectory Model Analysis

We cannot know precisely how the dust was transported since the tracer model was an Eulerian analysis. Thus trajectory analysis still plays a complementary role to the tracer model, although we must keep in mind the accuracy limitations due to the coarse grid and time intervals of the global data obtained. We utilized the Trajectory Analysis Model (EORC-TAM) developed by the Earth Observation Research Center (EORC) of the National Space Development Agency of Japan (NASDA) for the analysis [*Matsuzono et al.*, 1998], and EC-MWF global atmospheric data (the resolutions of grid and time were $2.5° \times 2.5°$ and 12 hours). The second-order Runge-Kutta method was used for the time integral of the differential equations of particle motion. We can perform both an insentropic analysis and an analysis using the vertical wind to trace the height of an air mass.

We performed a number of backward and forward trajectory analyses based primarily on the lidar observations (information of the dust height). We uncovered the apparent effects of the cutoff low at Hefei and Nagasaki when the cutoff low passed over those regions, e.g., a strong downward motion, a counterclockwise curved trajectory, and a confined motion at low levels. We will show here an example of the relations among the lidar observations and the source of the Asian dust. In Figure 10 we show the 5-day backward trajectories started from 1230 UTC, April 20, 1998, at an altitude of 2500 m over several Japanese sites. The altitude was taken after the simultaneous lidar observations shown in Figure 5. The vertical wind given by the ECMWF was used for the height determination (the result with the isentropic condition was similar). We can see that all the trajectories trace back to the source regions (near the Gobi desert) within 4 days. A careful examination of the results reveals that the effect of the cutoff low can still be seen in the trajectory from Nagasaki; it curved over the East China Sea and passed over near Hefei. This result coincided with the lidar observation at Hefei (Figure 3). Thus we can presume that the dust that passed near Hefei was trapped in the vortex and reached the south of Japan. In contrast, the dust that arrived over the main island of Japan passed mostly over the Korean peninsula. This also agrees with the lidar observations in Seoul (Figure 4). The trajectory from Sapporo appears to demonstrate a pass that differs from the above two behaviors.

A back trajectory analysis on the thin dust layer observed around 6 to 8 km at the same time (Figure 5) revealed that the air mass also traced back to near the source region, but within 2 days. This fact indicates that the air mass traveled faster at a higher altitude than at a lower one during the event. Therefore we must consider such a time lag when we examine the multilayered structure of Asian dust that is frequently observed.

5. Discussions

5.1. Cutoff Low and Asian Dust

This might be the first study on the effect of a cutoff low on Asian dust. A cutoff low has several interesting meteorological features, including the cold air mass, the strong sedimentation inside the vortex, the slow movement, and the driving down of the tropopause [*Palmén*, 1951; *Ogura*, 1993]. The ground-based and satellite observations and the model simulation demonstrated that the cutoff low brought the dense Asian dust epi-

sode by trapping the dust while it was traveling. The dust height remained below about 3 km during the episode except in the beginning, which was observed by the lidar network in Japan and also appeared in the model calculation. The dust height observed in Hefei and Seoul was somewhat higher than in Japan. After dissipation of the cutoff low over the Pacific on April 19, 1998, the subsequent high-pressure system might have continuously brought a downward current, or the dust might be mainly transported in the PBL from the southwest. The mechanism is complicated and more studies are required to clarify it.

5.2. Importance of Ground-Based Network Observations

The Asian dust that occurred in April of 1998 was observed widely in East Asia. Asian dust events are frequently observed in the southwest of Japan, but heavy dust was observed even in Sapporo during the event of April 1998, as indicated by the sky radiometer data (Figure 6). The images of SeaWiFS indicate that the main part of the Asian dust that reached the West Coast of the United States passed over the northern part of Sapporo [*Husar et al.*, this issue].

Our study of Asian dust using network operation is in an early stage. However, it shows promise for understanding the details of the transport mechanism of Asian dust using the model simulation presented here. The present model gives comprehensive information about the dust, including any temporal change of the surface concentration, the vertical height distribution of the dust at selected sites, and the horizontal distribution of the column dust concentration. Those elements are then compared with the ground-based and satellite observations. In a sense, each observation functions as a piece of a jigsaw puzzle of the overall image of the Asian dust. The observation and the model generally complement each other. The observation is factual and therefore valuable but limited in space and time, while the model can cover a wide area and time series but requires validation by observation. The lidar network is a powerful tool that provides a time-to-height cross section of the dust concentration in three dimensions, which thus raises the standards for the model results.

5.3. Role of the Thin Dust Layer in the Upper Atmosphere

The continuous measurement by the polarization lidar at TUMM on April 20 shows that the layer can be traced back to a cirrus cloud from an earlier time (Plate 2). The cirrus and dust apparently coexisted at that time, although the signal-to-noise ratio in the depolarization ratio is too low to discuss this quantitatively, as shown in Plate 2b. The air temperature where the cirrus existed (higher than 9 km in altitude) was below $-40°C$. Cirrus apparently tends to appear at the top region of a thin dust layer. *Sassen* [1999] introduced another example of TUMM polarization lidar data that suggested a dust-cirrus interaction on March 19, 1998. Thus we can infer that Asian dust acts as the ice nuclei of a cirrus cloud in the upper troposphere [*Isono et al.*, 1959]. A thin dust layer in the high troposphere was also seen in the observations of Hefei (Figure 3). The peak concentration of the thin dust layer in Hefei was on the same order as the dust layer observed in Japan; that is, the extinction coefficient was of the order of 0.01 km^{-1}, which can be converted to $R = 1.5$ at an altitude of about 8 km with $S_1 = 50$. The partial optical depth integrated from 6 to 12 km in altitude in Figure 3 was 0.026 and 0.054 for April 16 and 18, 1998. The model simulation also indicated an extended distribution to the high troposphere as seen in Plate 5. Thus the dust

in the higher troposphere injected by Asian dust events was small in optical thickness but would have a significant impact on the Earth's radiation budget when we consider its role in cirrus formation. The cirrus cloud is considered to be a highly uncertain component of the climate system [e.g., *Sassen*, 1997]. Polarization lidar is quite useful for studying the dust-cirrus interaction with high temporal resolution.

6. Conclusion and Summary

We explored a ground-based network observation of Asian dust in the east Asia region and successfully observed the huge Asian dust event that occurred in April 1998. The on-line transport model fairly well reproduced the observations of the vertical distribution of dust obtained by the lidar, the horizontal distribution of the dust concentration derived from NOAA/AVHRR, and the surface dust concentration given by OPC and PM_{10}. The simulation and the trajectory analysis led us to conclude that the effect of the cutoff vortex was responsible for the dust episode, especially in the southern part of Japan during the early stage. The transport height was below 3 km in the middle of Japan. The associated subsistence of the potential temperature under the traveling high must have caused the lower dust height, even after dissipation of the vortex into the Pacific east of Tokyo on April 19. The dust that passed near Hefei was apparently involved in the vortex. The air mass over Korea might have passed over the southwest of Japan.

We have provided direct evidence by polarization lidar observation that Asian dust interacts with cirrus. "A night with a hazy moon" (Oborozukiyo in Japanese) is used as a spring season word in haiku in Japan. This meteorologically implies that optically thin clouds like cirrus appear more often in the spring than in other seasons. Asian dust might have been enhancing cirrus activity in the spring since ancient times.

The successful ground-based network observations of Asian dust during the spring from 1997 to 1999 should encourage further extension of the network toward the inner region of the Asian continent, i.e., near the dust source region and Pacific Rim regions, to resolve global climate issues.

References

Angström, A., Techniques of determining the turbidity of the atmosphere, *Tellus*, *13*, 214–223, 1961.

Ansmann, A., M. Riebesell, U. Wandinger, C. Weitkamp, E. Voss, W. Lahmann, and W. Michaelis, Combined Raman elastic-backscatter LIDAR for vertical profiling of moisture, aerosol extinction, backscatter, and LIDAR ratio, *Appl. Phys.*, *B55*, 18–28, 1992.

Arao, K., and Y. Ishizaka, Volume and mass of yellow sand dust in the air over Japan as estimated from atmospheric turbidity, *J. Meteorol. Soc. Jpn.*, *64*, 79–94, 1986.

Arao, K., and C. Sakaguchi, Yellow sand events measured by an optical particle counter at Nagasaki University in 1996–1998 (in Japanese), *J. Environ. Stud. Nagasaki University*, *1*, 175–186, 1999.

Bates, T. S., B. J. Huebert, J. L. Gras, B. Griffiths, and P. A. Durkee, The International Global Atmospheric Chemistry (IGAC) project's first Aerosol Characterization Experiment (ACE 1)—Overview, *J. Geophys. Res.*, *103*, 16,297–16,318, 1998.

Fernald, G. F., Analysis of atmospheric lidar observations: Some comments, *Appl. Opt.*, *23*, 652–653, 1984.

Fukushima, H., T. Ohtake, M. Toratani, I. Uno, and B. J. Sohn, Distribution of Asian dust aerosol around Japan and over the Pacific estimated from the SeaWiFS data in April, 1998 (in Japanese), *Conf. Remote Sens. Soc. Jpn.*, *27*, 39–40, 1999.

Gillette, D., A wind tunnel simulation of the erosion of soil: Effect of soil texture, sand-blasting, wind speed, and soil consolidation on the dust production, *Atmos. Environ.*, *12*, 1735–1743, 1978.

Hu, H., J. Zhou, and Y. Wu, Lidar measurements of stratospheric aerosol over Hefei, China during 1991–1996, *Proc. SPIE*, vol *3504*, 184–186, 1998.

Husar, R. B., et al., Asian dust events of April 1998, *J. Geophys. Res.*, this issue.

Imasu, R., Determination of high concentration area of atmospheric aerosols using 2 channel satellite infrared images (in Japanese), *Aerosol Res.*, *7*, 125–134, 1992.

Inoue, T., The relationship of sea surface temperature and water vapor amount to convection over the western tropical Pacific revealed from split window measurements, *J. Meteorol. Soc. Jpn.*, *68*, 589–606, 1990.

Isono, K., M. Komabayashi, and A. Ono, The nature and origin of ice nuclei in the atmosphere, *J. Meteorol. Soc. Jpn.*, *37*, 211–233, 1959.

Iwasaka, Y., H. Minoura, and K. Nagaya, The transport and spatial scale of Asian dust-storm clouds: A case study of the dust-storm event of April 1979, *Tellus*, *35B*, 189–196, 1983.

Iwasaka Y., M. Yamato, R. Imasu, and A. Ono, Transport of Asian dust (KOSA) particles; Importance of weak KOSA events on the geochemical cycle of soil particles, *Tellus, Ser. B*, *40*, 494–503, 1988.

Jinhuan, Q., and S. Jinhui, Optically remote sensing of the dust storm and the analysis, *Chinese J. Atm. Sci.*, *18*, 1–10, 1994.

Kai, K., Y. Okada, O. Uchino, I. Tabata, H. Nakamura, T. Takasugi, and Y. Nikaidou, Lidar observation of a Kosa (Asian dust) over Tsukuba, Japan during the spring of 1986, *J. Meteorol. Soc. Jpn.*, *66*, 457–472, 1988.

Kinoshita, K., M. Nishinosono, T. Yano, N. Iino, and I. Uno, Detection and analysis of Kosa using NOAA/AVHRR data (in Japanese), *Conf. Remote Sens. Soc. Jpn.*, *26*, 253–256, 1999.

Kobayashi, A., S. Hayashida, K. Okada, and Y. Iwasaka, Measurements of the polarization properties of KOSA (Asian dust storm) particles by a laser radar in spring 1983, *J. Meteorol. Soc. Jpn.*, *63*, 144–149, 1985.

Lee, H. S., I. H. Hwang, J. D. Spinhirne, and V. S. Scott, Micropulse lidar for aerosol and cloud measurement, in *Advances in Atmospheric Remote Sensing With Lidar*, edited by A. Ansmann, R. Neuber, P. Rairoux, and U. Wandinger, pp. 7–10, Springer-Verlag, New York, 1997.

Liu, Z., I. Matui, N. Sugimoto, High-spectral-resolution lidar using an iodine absorption filter for atmospheric measurements, *Opt. Eng.*, *38*, 1661–1670, 1999.

Matsui, I., and N. Sugimoto, Continuous measurement of tropospheric aerosols and clouds with a compact Mie scattering lidar, *Tech. Dig.*, *CLEO/Pacific Rim '97*, Chiba, Japan, 235, 1997.

Matthews, E., Global vegetation and land use: New high-resolution data bases for climate studies, *J. Clim. Appl. Meteorol.*, *22*, 474–487, 1983.

Matuzono, T., T. Sano, and T. Ogawa, Development of the trajectory analysis model (EORC-TAM), *EORC Techn. Rep.*, *1*, 55–68, 1998.

Murayama, N., Dust cloud "Kosa" from the east Asian dust storms in 1982–1988 as observed by the GMS satellite, *Meteorol. Satell. Cent. Tech Note*, *17*, 1–8, 1988.

Murayama, T., M. Furushima, A. Oda, N. Iwasaka, and K. Kai, De-

Murayama, T., et al., Lidar network observation of Asian dust (Asian dust) in Japan, *Proc. SPIE*, *3504*, 8–15, 1998.

Murayama, T., H. Okamoto, N. Kaneyasu, H. Kamataki, and K. Miura, Application of lidar depolarization measurement in the atmospheric boundary layer: Effects of dust and sea-salt particles, *J. Geophys. Res.*, *104*, 31,781–31,792, 1999a.

Murayama, T., et al., Lidar network observation of Asian dust over Japan in 1999 Spring (abstract), *Int. Laser Sens. Symp.*, *20th*, 29–32, 1999b.

Nakajima, T., M. Tanaka, M. Yamano, M. Shiobara, K. Arao, Y. Nakanishi, Aerosol optical characteristics in the yellow sand events observed in May, 1982 at Nagasaki, part II, Models, *J. Meteorol. Soc. Jpn.*, *67*, 269–291, 1989.

Nakajima, T., G. Tonna, R. Rao, P. Boi, Y. Kaufman, and B. Holben, Use of sky brightness measurements from ground for remote sensing of particulate polydispersions, *Appl. Opt.*, *35*, 2672–2686, 1996.

Niimura, N., K. Okada, X. B. Fan, K. Kai, K. Arao, G. Y. Shi, and S. Takahashi, Formation of Asian dust-storm particles mixed internally with sea salt in the atmosphere, *J. Meteorol. Soc. Jpn.*, *76*, 275–288, 1998.

Ogura, Y., Kminari to seturi-teikiatsu (in Japanese), *Kisho*, *37(6)*, 32–35, 1993.

Palmén, E., The aerology of extratropical disturbances, in *Compendium of Meteorology*, edited by T. F. Malone, pp. 599–620, Am. Meteorol. Soc., Boston, Mass., 1951.

Pielke, R. A., et al., A comprehensive meteorological modeling system—RAMS, *Meteorol. Atmos. Phys.*, *49*, 69–91, 1992.

Pollack, J. B., and J. N. Cuzzi, Scattering by nonspherical particle size comparable to a wavelength: A new semi-empirical theory and its application to tropospheric aerosols, *J. Atmos. Sci.*, *37*, 868–881, 1980.

Prata, A. J., Observations of volcanic ash clouds in the 10–12 micro in window using AVHRR/2 data, *Int. J. Remote Sens.*, *10*, 751–761, 1989.

Sakai, T. T. Shibata, S. A. Kwon, Y. S. Kim, K. Tamura, and Y. Iwasaka, Free tropospheric aerosol backscatter, depolarization ratio, and relative humidity measured with the Raman lidar at Nagoya in 1994–1997: Contributions of aerosols from the Asian continent and Pacific Ocean, *Atmos. Environ.*, *34*, 431–442, 2000.

Sassen, K., Contrail-cirrus and their potential for regional climate change, *Bull. Am. Meteorol. Soc.*, *78*, 1885–1903, 1997.

Sassen, K., The lidar backscatter depolarization technique for cloud and aerosol research in *Light Scattering by Nonspherical Particles: Theory, Measurements, and Geophysical Applications*, edited by M. L. Mishchenko, J. W. Hovenier, and L. D. Travis, pp. 393–416, Academic, San Diego, Calif., 1999.

Shibata, T., T. Sakai, M. Hayashi, T. Ojio, S. A. Kwon, and Y. Iwasaka, Raman lidar observations: Simultaneous measurements of water vapor, temperature and aerosol vertical profiles, part I, *J. Geomagn. Geoelectr.*, *48*, 1127–1135, 1996.

Shipley, S. T., D. H. Tracy, E. W. Eloranta, J. T. Trauger, J. T. Sroga, F. L. Roesler, and J. A. Weinman, High spectral resolution lidar to measure optical scattering properties of atmospheric aerosols, 1, Theory and instrumentation, *Appl. Opt.*, *22*, 3716–3724, 1983.

Sokolik, I. N., and O. B. Toon, Direct radiative forcing by anthropogenic airborne mineral aerosols, *Nature*, *381*, 681–683, 1996.

Spinherne, J. D., Compact eye safe lidar systems, *Rev. Laser Eng.*, *23*, 112–118, 1995.

Takashima, T., and K. Masuda, Emissivity of quartz and Sahara dust powders in the infrared region (7–17 μm), *Remote Sens. Environ.*, *23*, 51–63, 1987.

Tanaka, M., M. Shiobara, T. Nakajima, M. Yamano, and K. Arao, Aerosol optical characteristics in the yellow sand events observed in May, 1982 at Nagasaki, part I, Observations, *J. Meteorol. Soc. Jpn.*, *67*, 267–278, 1989.

Tanaka, T., Kannreiuzu to Kosa (in Japanese), *Kisho*, *42*, 6, 20–21, 1998.

Tegen, I., A. A. Lacis, and I. Fung, The influence on climate forcing of mineral aerosols from disturbed soils, *Nature*, *380*, 419–422, 1996.

Uematsu, M., R. A. Duce, J. M. Prospero, L. Chen, J. T. Merrill, and R. L. McDonald, Transport of mineral aerosol from Asia over the North Pacific Ocean, *J. Geophys. Res.*, *88*, 5343–5352, 1983.

Yoon, S. C., and J. G. Won, Monitoring of atmospheric aerosols in

Seoul using a micropulse lidar, in *19th International Laser Radar Conference*, *NASA/CP-1998-207671/PT1*, pp. 83–85, 1998.

Whiteman, D. N., S. H. Melfi, and R. A. Ferrare, Raman lidar system for the measurement of water vapor and aerosols in the Earth's atmosphere, *Appl. Opt.*, *31*, 3068–3082, 1992.

Yoon, S. C., J. G. Jhun, and J. G. Won, Aerosol and yellow-sand monitoring with a micropulse lidar in Seoul, *Tech. Dig.*, *CLEO/Pacific Rim '99*, Seoul, Korea, 1054–1055, 1999.

Zhou, J., Optical properties of tropospheric aerosols derived from lidar measurements over Hefei, *Proc. SPIE*, *3501*, 112–117, 1998.

———————

N. Hagiwara and T. Murayama, Department of Physics, Tokyo University of Mercantile Marine, 2-1-6 Etchujima, Koto, Tokyo, Japan. (murayama@ipc.tosho-u.ac.jp)

Z. Liu, I. Matsui, and N. Sugimoto, Atmospheric Environment Division, National Institute for Environmental Studies, Tsukuba, Ibaraki, Japan.

I. Uno, Research Institute for Applied Mechanics, Kyushu University, Kasuga, Fukuoka, Japan.

K. Kinoshita, Faculty of Education, Kagoshima University, Kagoshima, Japan.

K. Aoki, Institute of Low Temperature Science, Hokkaido University, Sapporo, Hokkaido, Japan.

Y. Iwasaka, T. Sakai, and T. Shibata, Solar-Terrestrial Environment Laboratory, Nagoya University, Chikusa, Nagoya, Aichi, Japan.

K. Arao, Faculty of Environmental Studies, Nagasaki University, Nagasaki, Japan.

B.-J. Sohn, Department of Earth Sciences, Seoul National University, Seoul, Korea.

J.-G. Won and S.-C. Yoon, Department of Atmospheric Sciences, Seoul National University, Seoul, Korea.

H. Hu, T. Li, and J. Zhou, Anhui Institute of Optics and Fine Mechanics, Hefei, Anhui, China.

M. Abo, Graduate School of Electrical Engineering, Tokyo Metropolitan University, Tokyo, Japan.

K. Iokibe and R. Koga, Faculty of Engineering, Okayama University, Okayama, Japan.

18,360